



## Application of harmony search algorithm to evaluate performance of diamond wire saw

R. Mikaeil<sup>1\*</sup>, Y. Ozcelik<sup>2</sup>, M. Ataei<sup>3</sup> and S. Shaffiee Haghshenas<sup>4</sup>

1. Department of Mining and Metallurgical Engineering, Urmia University of Technology, Urmia, Iran

2. Hacettepe University, Department of Mining Engineering, Ankara, Turkey

3. School of Mining, Petroleum & Geophysics Engineering, Shahrood University of Technology, Shahrood, Iran

4. Young Researchers and Elite Club, Rasht Branch, Islamic Azad University, Rasht, Iran

Received 5 July 2016; received in revised form 2 September 2016; accepted 24 September 2016

### Keywords

Dimension Stone

Diamond Wire Saw

Wear Rate

Harmony Search Algorithm

### Abstract

Evaluation and prediction of performance of diamond wire saw is one of the most important factors involved in planning the dimension stone quarries. The wear rate of diamond wire saw can be investigated as a major criterion to evaluate its performance. The wear rate of diamond wire saw depends upon non-controlled parameters related to rock characteristics and controlled parameters related to characteristics of the cutting machine and operational parameters. Under the same working conditions, the wear rate of diamond wire saw is strongly affected by the rock properties. This is a key factor that required in evaluating the wear rate of diamond wire saw. In this work, the four major dimension stone properties uniaxial compressive strength, Schimazek F-abrasivity factor, Shore hardness, and Young's modulus were selected as the criteria to evaluate the wear rate of diamond wire saw using the harmony search algorithm (HSA). HSA was used to cluster the fifteen different andesite quarries located in Turkey. The studied dimension stones were classified into three classes. The results obtained show that the algorithm applied can be used to classify the performance of diamond wire saw according to its wear rate by only some famous physical and mechanical properties of dimension stone.

### 1. Introduction

Nowadays, diamond wire saw is one of the most important tools used in the stone quarries. Predicting the sawability of dimension stone is very important in planning the dimension stone quarries. Up to the present time, diamond wire cutting has been well-reported in the literature [1-13]. Özçelik has investigated the working conditions of diamond wire-cutting machines in the marble industry [1]. Similarly, Özçelik and Kulaksız have studied the wear of diamond wire saw. They have investigated the relationship between the cutting angles and the wear on beads in the diamond wire-cutting method [2, 3]. Özçelik has analysed the wear on diamond beads in the cutting of andesitic rocks using the multivariate statistical analysis [4]. Özçelik et al.

have investigated the effects of the mineralogical, petrographical, and textural properties on marble cuttings with diamond wire [5, 6, 8]. Mikaeil et al. have studied the relationship between the production rate and the rock properties in carbonate rock cuttings with diamond wire saw [9]. Ataei et al. have developed the statistical models to predict the production rate of diamond wire saw in carbonate rock cuttings [10]. Ghaysari et al. have investigated the performance of diamond wire saws with respect to the textural characteristics of rocks [11]. Sadegheslam et al. have predicted the production rate of diamond wire saws using the multiple non-linear regression analysis and the artificial neural network [12]. Almasi et al. have investigated the effects of

✉ Corresponding author: [reza.mikaeil@uut.ac.ir](mailto:reza.mikaeil@uut.ac.ir) (R. Mikaeil).

cutting wire tension on the Travertine cutting rate [13].

A diamond wire is simply a steel cable on which small beads bonded with diamond abrasive are mounted at regular intervals with spacing material placed between the beads [5]. Briefly, in a diamond wire cutting, the holes vertical, horizontal, and perpendicular to each other are drilled through the block. A horizontal hole is drilled to remove the gravity effect of a block. After that, vertical holes are performed. The initial step for a vertical cutting is to drill two holes that intersect at a 90° angle. Then the diamond wire is threaded through these holes and mounted around

the drive wheel of the diamond wire cutting machine, and the two ends of the wire are clamped together. The diamond wire is rotated via the movement of a drive wheel. The tension and rotation force required for cutting is provided by the movement of the diamond wire cutting machine away from the cut surface on the rail. Water is supplied during the diamond wire cutting operation both as a coolant and as a means of removing waste particles [5]. The schematic presentation of a diamond wire-cutting layout and cross-section of diamond bead are illustrated in Figure 1.

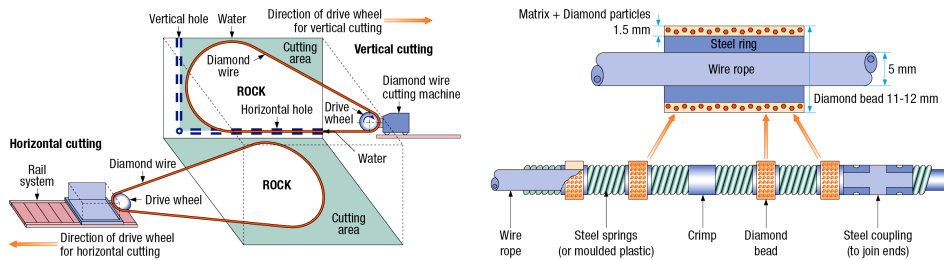


Figure 1. Schematic presentation of a diamond wire-cutting layout and cross-section of diamond bead [1].

In the rock sawing mechanism, chip formation may be defined as the destruction of a work-piece material using diamond particles on the segment surface. This process is a grinding one. The diamond particles remove the material through scratching and cracking the work-piece surface. Wire sawing is a grinding process with impregnated or electroplated diamonds, and can be compared with grinding as an abrasive process. As shown in Figure 2, the cutting mechanism during grinding of metals has been thoroughly explained by Tonshoff and Hillmann [14]. The diamond wire sawing mechanism is similar to the dimension stone cutting process mechanism, in which there are three main parts of the cutting process during tool engagement for the point-of-cutting action of a single diamond grit. Angle  $\eta$  is the cutting edge of the grit impinges

on the work-piece surface. In the first main area (I), elastic deformation appears. Friction between the work-piece and the diamond grit increases the temperature. In area II, according to penetration of the grit into the material, plastic material deformation also occurs. The friction and resilience cause an increase in the temperature in the near-surface area of the work-piece. Thus the elastic limit of the material is reduced, and the plastic deformation of the material is promoted. Subsequently, the topography of the material surface is greatly changed, i.e. as material buckling. The main part of the grinding process occurs in zone III, where the chip is generated. Shear processes generate heat during the chip building process, with plastic displacement occurring at the same time [14].

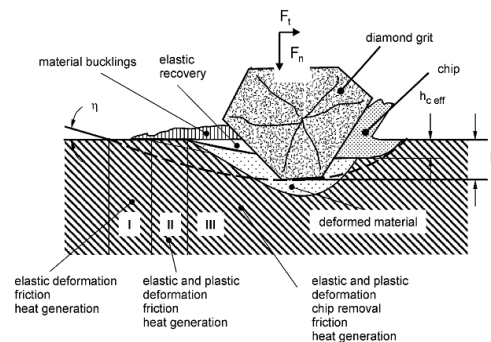


Figure 2. Cutting mechanism during grinding of metal material [14].

In this work, it is aimed to evaluate the performance of a diamond wire saw according to the physical and mechanical properties of the sawn dimension stone. Evaluation of the performance of a diamond wire saw may be used for cost analysis and project planning as a decision-making index. According to the authors' knowledge, evaluating the performance of a diamond wire saw in terms of wear rate using the meta-heuristic algorithm is a unique research work.

## 2. Factors affecting wear rate of diamond wire saw

The performance of a diamond wire saw in term of wear rate depends upon non-controlled parameters related to the rock characteristics and controlled parameters related to the sawing tools and equipment and working conditions. These parameters are listed in Table 1.

**Table 1. Factors affecting sawability of dimension stones [1].**

Non-controlled parameters related to rock characteristics	Partially-controlled or controlled parameters	
	Properties of sawing tools and equipment	Working conditions
Hardness	Machine position and power	Technical personnel
Abrasiveness	Number of beads per meter	Vibration of machine
Strength	Bead structure	
Water content	Diamond and matrix properties	
Degree of alteration	Amount of cutting area with respect to angle variation	
Discontinuities	Wire speed	
Mineralogical properties	Amount of water used	
Textural characteristics	Cutting angle between wire and horizontal level	
	Dimensions of block	

Under the same working conditions, the wear rate is affected by the physical and mechanical properties of rocks. It is obvious that different rocks have different properties, which produce different performances for the diamond wire saw. In order to develop a new classification system, selecting the most effective parameters and a combination of them in a unique structure are the important issues. In rock classification systems, as a very important and basic rule, the number of parameters used should be small. Therefore, using all parameters is inconvenient from the practical and engineering viewpoints. In addition, some of the parameters involved have no comprehensive and quantitative laboratory test (scale). Thus in a practical classification system, to select the final major parameters (tests), two assumptions have been considered:

(a) The number of parameters used should be small, and (b) Equivalent parameters should be avoided. According to these assumptions, the four parameters (standard tests) uniaxial compressive strength, Schimazek F-abrasivity factor, Shore hardness, and Young's modulus were chosen to evaluate the performance of a diamond wire saw. Uniaxial compressive strength is one of the most important engineering properties of rocks. Abrasiveness is one of the most effective factors that influence the tool wear. Abrasiveness is

mainly affected by the factors mineral composition, hardness of mineral constituents, and grain characteristics such as size, shape, and angularity. In this research work, Schimazek's F-abrasiveness was selected as the abrasiveness factor. This factor depends on the textural and mechanical properties, and has a good ability for evaluating the rock abrasivity. The F-abrasivity factor is defined as:

$$F = \frac{EQC \times G_s \times BTS}{100} \tag{1}$$

where F is the Schimazek's wear factor (N/mm), EQC is the equivalent quartz content percentage, G<sub>s</sub> is the median grain size (mm), and BTS is the indirect Brazilian tensile strength.

Hardness can be interpreted as the rock resistance to penetration. According to rock behavior during the fracture process, especially in sawing, the way that rocks reach the failure point (primary chip formation) has a great influence on the wear rate of diamond and matrix. The best scale for rock elasticity is the Young's modulus. Based on the ISRM suggested methods [15], the tangent Young's modulus at a stress level equal to 50% of the ultimate uniaxial compressive strength is used in this ranking system.

### 3. Studied areas

The studied areas were the andesite quarries located in the western side of Menekse Hill, in the Çubuk district, 60 km NE of Ankara, the capital of Turkey. The location map of the andesite quarries is given in Figure 3. It occurs in the Tertiary Mamak Formation, which consists of volcanic units such as andesite, dacite, rhyolitic lava, and tuff. According to the thin section studies performed on the andesite samples taken from different parts of the studied area, andesite has microlitic hyaline, as a matrix, and shows a porphyritic texture. In the thin sections of the rock, plagioclase, biotite, hornblende, quartz, matrix, and opaque minerals are determined in each thin section. The Ankara andesitic rocks used in the study had a porphyritic texture. In its structure, the plagioclase content varies between 15.8 and 26.8, the biotite content varies between 0.8 and 2.5, the hornblende content varies between 0.1 and 1.8, the quartz content varies between 1.0 and

7.0, the matrix content varies between 68.5 and 74.8, and the opaque minerals content varies between 0.3 and 1.2. Generally, they show current layering in decimetric thicknesses. These are defined by the grain size of minerals and the slight changes in color. The position of the lava flow varies between N30–35E and 26–45SE in the center of the deposit and on the northern part. In the southern part, a significant difference is observed. The strike is between E–W and N63W. The dip is between 37° and 55° towards north and NE. Andesite has a compact structure and a microscopic reddish brown color from light to dark because of the variation in the amount of minerals and the chemical composition in the matrix. Since the plagioclase crystals, ferric minerals (FeO, Fe<sub>2</sub>O<sub>3</sub>), and andesite enclaves are centimeters in size, they have a bright appearance. Andesite is covered with a layer of soil. The extraction of andesite blocks is achieved by diamond wire sawing [16, 17].

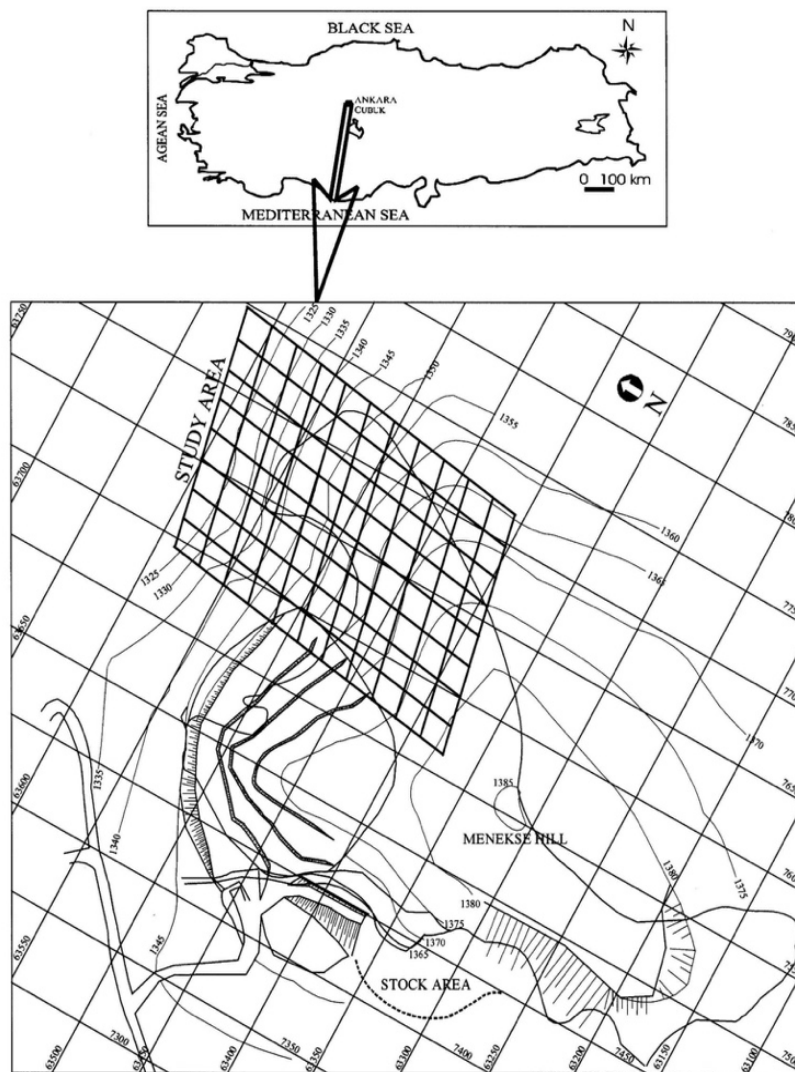


Figure 3. Location map of andesite quarries and studied area.

#### 4. Laboratory tests

Laboratory tests were performed to determine the mentioned physical and mechanical properties of the studied dimension stone. The dimension stone block samples were collected from 15 different andesite quarries. Each block sample was inspected for macroscopic defects so that it would provide test specimens free from fractures,

partings or alteration zones. Then the test samples were prepared from these block samples, and the standard tests were completed to measure the above-mentioned parameters following the suggested procedures by the ISRM standards [15]. The results obtained from the field and laboratory studies are listed in Table 2.

**Table 2. Result of laboratory and field studies.**

Rock samples		UCS MPa	BTS MPa	EQC %	Gs $\mu\text{m}$	SF-a N/mm	YM GPa	SH N
1	Andesite1	28.05	3.72	2.00	135.00	0.01004	6.80	33.00
2	Andesite2	47.39	5.05	2.00	130.00	0.01313	7.60	39.93
3	Andesite3	77.25	9.55	3.00	115.00	0.03295	20.80	65.00
4	Andesite4	84.02	8.86	3.00	110.00	0.02924	23.50	63.62
5	Andesite5	26.55	3.56	1.00	124.00	0.00441	7.90	49.93
6	Andesite6	67.41	9.83	5.00	108.00	0.05308	15.50	67.00
7	Andesite7	57.75	6.15	2.00	140.00	0.01722	8.00	43.70
8	Andesite8	87.53	8.82	7.00	51.00	0.03149	30.56	61.38
9	Andesite9	75.75	9.25	5.00	53.00	0.02451	24.60	63.70
10	Andesite10	81.35	9.20	5.50	58.00	0.02935	25.40	62.48
11	Andesite11	78.75	8.95	4.00	76.00	0.02721	26.40	60.30
12	Andesite12	82.50	9.10	4.20	85.00	0.03249	28.30	61.20
13	Andesite13	27.23	3.68	3.00	115.00	0.01270	7.30	42.50
14	Andesite14	51.92	5.53	2.80	131.00	0.02028	7.76	41.20
15	Andesite15	56.25	6.05	3.00	120.00	0.02178	8.01	43.50

UCS: Uniaxial Compressive Strength, BTS: Brazilian Tensile Strength, EQC: Equivalent quartz content, Gs: Grain size, SF-a: Schmiatzek F-abrasivity factor, YM: Young's Modules, SH: Shore hardness, Wr: Wear rate

#### 5. Harmony search algorithm

Soft computing approaches such as the fuzzy sets and fuzzy logic, meta-heuristic algorithms, and neural networks (NNs) are used as the predictive tools [18-24]. The Harmony search (HS) algorithm is a powerful tool for identifying and assessing complex systems as one of the soft computing techniques. HS was first proposed by Geem [25] and used to solve the optimization problem of water distribution networks. As a novel population-based meta-heuristic algorithm, during the recent years, it has gained a great research success in the areas of mechanical engineering, control, and signal processing [26-31].

The HS algorithm includes the following steps [32]:

Step 1: Initialize the HS memory.

The initial HM consists of a given number of randomly-generated solutions to the optimization problems under consideration.

Step 2: Create a new solution from HM.

Step 3: Update HM.

The new solution from Step 2 is evaluated. If it yields a better fitness than that of the worst member in HM, it will replace that one. Otherwise, it is eliminated.

Step 4: Repeat Step 2 to Step 3 until a preset termination criterion, e.g. the maximal number of iterations, is met.

Figure 4 shows the flowchart of the basic HS algorithm.

#### 6. Application of HSA to evaluate wear rate of dimension stone

For modeling and assessment of the laboratory test results using HSA and the clustering technique, first the pseudo-code of the algorithm is determined according to the algorithm process in the flowchart of Figure 3 and Equation (2).

$$\text{Obj.Function} = \sum_{i=1}^n \min_{1 \leq j \leq k} d(x_i, m_j) \quad (2)$$

where  $d$  is the Euclidean distance of a single data point ( $x_i$ ) to the cluster center ( $m_j$ ).

After the initial analysis and running the program for several times, the best control parameters are selected. The control parameters in the algorithm are considered as the minimum acceptance precision of  $\epsilon_L=0.00001$ , maximum iteration of 400, harmony memory size of 100, number of new harmony of 50, and harmony memory

consideration rate of 0.5. Furthermore, the number of clusters is considered to be 3 based on the supervised classification. The algorithm works with input data, and it is independent from the output data in the clustering technique. At the end, the laboratory test results are normalized and prepared for analysis and modeling as input data using pseudo-codes in Matlab software. In Tables 3 and 4, the optimization results for the classification are shown. According to the results tabulated in Table 3, the studied dimension stones were classified into three separate groups based on their physical and mechanical properties. The distances of the centers of the clusters from the criteria are given in Table 4. As it can be seen in this table, UCS and SH in the first class, SH and SF-a in the second class, and SH in the third class are the main criteria.

The precision level and calculation termination of HSA are given in Table 5. According to the results tabulated in this table, the algorithm converged in short iteration lengths from ninety four to four hundred iterations.

The minimum cost per iteration in HSA and the position of the samples in clustering by HSA for three clusters are illustrated in Figures 5 and 6. Figure 5 shows that computing is obtained the desired precision level of  $\epsilon_L$  and a suitable optimization is carried out by HSA in the 94<sup>th</sup> step and it is fixed from the 94<sup>th</sup> to the 400<sup>th</sup> iteration. Therefore, the calculations are stopped. The position of each data and centers of the clusters are illustrated in Figure 6.

**Table 3. Optimization and classification of samples by HSA for 3 clusters.**

Samples	Optimum partition of HSA			Classification of HSA	
A <sub>1</sub>	1.031	1.095	0.251	<b>First class</b>	A <sub>3</sub>
A <sub>2</sub>	0.833	0.923	0.039		A <sub>4</sub>
A <sub>3</sub>	0.178	0.431	0.748		A <sub>8</sub>
A <sub>4</sub>	0.071	0.559	0.802		A <sub>9</sub>
A <sub>5</sub>	0.988	1.095	0.328		A <sub>10</sub>
A <sub>6</sub>	0.583	4.8e-12	0.893		A <sub>11</sub>
A <sub>7</sub>	0.725	0.808	0.147		A <sub>12</sub>
A <sub>8</sub>	0.188	0.689	0.986	<b>Second class</b>	A <sub>6</sub>
A <sub>9</sub>	0.104	0.616	0.758	<b>Third class</b>	A <sub>1</sub>
A <sub>10</sub>	1.5e-11	0.583	0.821		A <sub>2</sub>
A <sub>11</sub>	0.067	0.628	0.807		A <sub>5</sub>
A <sub>12</sub>	0.113	0.608	0.909		A <sub>7</sub>
A <sub>13</sub>	0.956	0.993	0.219		A <sub>13</sub>
A <sub>14</sub>	0.759	0.794	0.121		A <sub>14</sub>
A <sub>15</sub>	0.71	0.735	0.185		A <sub>15</sub>

**Table 4. Distance of cluster centers from criteria by HSA for 3 clusters.**

	C <sub>1</sub>	C <sub>2</sub>	C <sub>3</sub>
<b>UCS</b>	0.929	0.77	0.526
<b>SH</b>	0.933	1	0.614
<b>SF-a</b>	0.547	1	0.276
<b>YM</b>	0.831	0.507	0.25

**Table 5. Precision level and calculation termination of HSA.**

Precision level and calculation termination of HSA				
Step (n)	$U^{(n-1)}$	$U^{(n)}$	$\epsilon_L = U^{(n)} - U^{(n-1)}$	Result
93	2.0159	2.0158	0.0001 > 0.00001	Continue
94	2.0158	2.0158	0 < 0.00001	Continue
400	2.0158	2.0158	0 < 0.00001	Stop

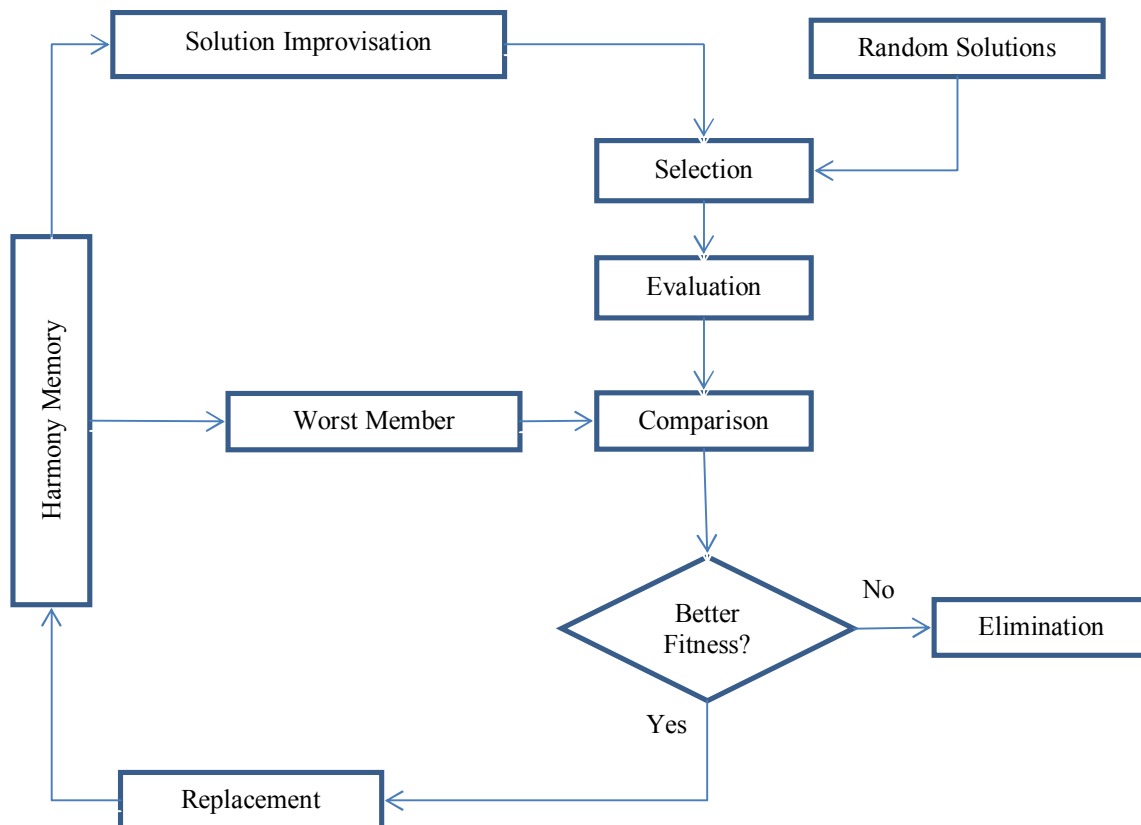


Figure 4. HS method [32].

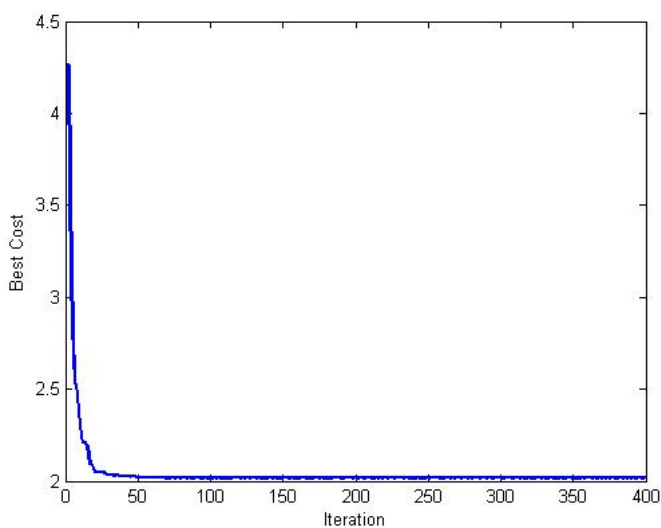


Figure 5. Minimum cost per iteration in HSA.

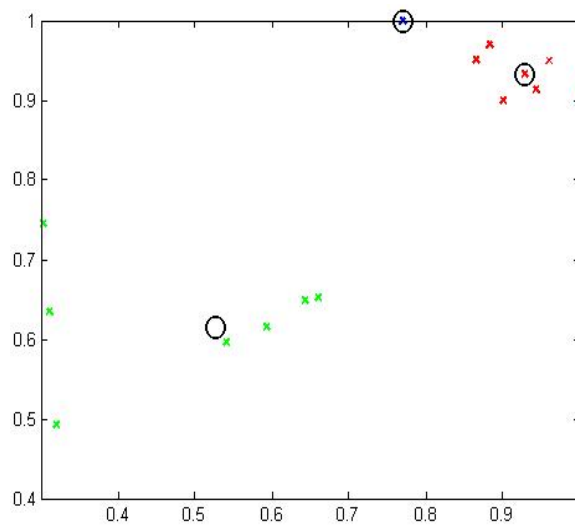


Figure 6. Position of samples in clustering by HSA for three clusters.

Table 6. Fixed parameters of machines and equipment employed in this work.

Number of beads per meter	37
Power of the machine (kW)	37.3
Speed of machine (rpm)	750
Voltage (V)	380
Stretching amperage (A)	25
Pullback force (MPa)	3.6
Pulley diameter (cm)	80

**Table 7. Classification of studied dimension stones by HSA and comparison with wear rate.**

Rock sample	Classification by HAS			Wear rate (mm/m <sup>2</sup> )
	Class 1	Class 2	Class 3	
A <sub>1</sub> Andesite1			*	0.0015
A <sub>2</sub> Andesite2			*	0.0023
A <sub>3</sub> Andesite3	*			0.0036
A <sub>4</sub> Andesite4	*			0.0034
A <sub>5</sub> Andesite5			*	0.0021
A <sub>6</sub> Andesite6		*		0.005
A <sub>7</sub> Andesite7			*	0.0016
A <sub>8</sub> Andesite8	*			0.0157
A <sub>9</sub> Andesite9	*			0.0168
A <sub>10</sub> Andesite10	*			0.0159
A <sub>11</sub> Andesite11	*			0.0085
A <sub>12</sub> Andesite12	*			0.008
A <sub>13</sub> Andesite13			*	0.0036
A <sub>14</sub> Andesite14			*	0.0022
A <sub>15</sub> Andesite15			*	0.0036

### 7. Validation of applied algorithm

Clustering is one of the powerful data mining techniques that groups the samples that have similar features and builds a concept hierarchy. In this work, the performance of a diamond wire saw was classified into three classes based on some important physical and mechanical properties of dimension stones using HSA. For validation and verifying of the results of the applied algorithm, field studies were carried out. The wear rate of a diamond wire saw in cutting a dimension stone was selected as a criterion to evaluate and validate the applied algorithm. To determine the wear rate of the diamond wire saw, a field study and an experimental procedure were carried out. Field studies including block cutting operations using a diamond wire cutting machine were performed on fifteen different andesitic dimension stones in the andesite quarries located in Ankara, Turkey. At least, three cutting operations were performed for each andesitic dimension stone on site, and their averages were taken and recorded as a representative on-site measurement. Some of the machine parameters, given in Table 6, were fixed in order to achieve more correct results.

Bead diameters located in the diamond wire were measured before and after the cutting tests in order to determine the amount of wearing on the diamond beads in the field study. This wear was recorded as the difference in the diameter measurements using a three-digit digital micrometer. Wearing measurements were carried out containing at least 1/4 of the wire length used and taking at least four measurements from the different sides of a bead. Then the unit wear values of the beads were identified as the amount

of wear per square meter (mm/m<sup>2</sup>). The wear rate value and classification of the studied dimension stones by HSA are given in Table 7.

As it can be seen in Table 7, the studied dimension stones were classified into three classes. These classes have a good relationship with the wear rate of the diamond wire saw. A<sub>3</sub> and A<sub>4</sub>, with a wear rate of 0.0036, were placed in Class 1 because their rock properties were similar to the properties of the first class samples; although their wear rate was closer to the Class 3 samples. According to the results obtained, the wear rate of a diamond wire saw was divided into the following three ranges: 0-0.004 mm/m<sup>2</sup>, 0.004-0.007 mm/m<sup>2</sup>, and 0.007 mm/m<sup>2</sup> <wr (wear rate).

### 8. Conclusions

In this work, we presented an adaptive soft computing technique to address the non-controlled and controlled parameters related to the machine properties of an uncertain mechanical process. A meta-heuristic algorithm was developed for evaluating the performance of a diamond wire saw using an evolutionary technique like harmony search algorithm (HSA). During this research work, 15 different dimension stones belonging to the andesite group were cut in quarries on-site using a diamond wire cutting machine. The wear rate of the diamond wire saw was used to evaluate the ability of the classification algorithm. In addition, the fitness function was chosen to be the Loyd's algorithm (k-means clustering) in order to minimize the distances of a cluster member on all clusters and



maximize the distances between the centers of the clusters. It was concluded that HSA with an appropriate fitness function was precise enough to predict the performance of a diamond wire saw in terms of the wear rate of a dimension stone. As a finalized result, it seems that the applied algorithm can be primarily used to evaluate and get information about the wear rate of a diamond wire saw in sawing dimension stones at any stone quarry with different rocks based on their mechanical and physical properties such as the uniaxial compressive strength, Schmiarezek F-abrasivity factor, Shore hardness, and Young's modulus.

## References

- [1]. Özçelik, Y. (1999). Investigation of the working conditions of diamond wire cutting machines in marble industry. Ph.D. Thesis. Hacettepe University. Ankara. 242 P. (in Turkish with English Abstract).
- [2]. Özçelik, Y. and Kulaksız, S. (2000). Investigation of the relationship between cutting angles and wear on beads in diamond wire cutting method. 9<sup>th</sup> Mine Planning and Equipment Selection Symposium. Panagiotou & Michalakopoulos (Ed.). pp. 661-666.
- [3]. Özçelik, Y., Kulaksız, M.C. and Etin, C. (2002). Assessment of the wear of diamond beads in the cutting of different rock types by the ridge regression. J. Mater. Process. Technol. 127: 392-400.
- [4]. Özçelik, Y. (2003). Multivariate statistical analysis of the wear on diamond beads in the cutting of andesitic rocks Key Engineering Materials. 250: 118-130.
- [5]. Özçelik, Y., Polat, F. and Bayram, A.M. (2004). Investigation of the Effects of Textural Properties on Marble Cutting with Diamond wire. Int. J. Rock Mech. Min. Sci. 41 (1): 228-234.
- [6]. Özçelik, Y. (2005). Effect of Mineralogical and Petrographical Properties of Marble on Cutting by Diamond Wire. CIM Bulletin. 98 (1085): 1-6.
- [7]. Özçelik, Y. (2005). Optimum working conditions of diamond wire cutting machines in the marble industry. Industrial Diamond Review. 1: 58-64.
- [8]. Özçelik, Y. (2007). The effect of marble textural characteristics on the sawing efficiency of diamond segmented frame saws. Industrial Diamond Review. 1: 65-70.
- [9]. Mikaeil, R., Ataei, M. and Hoseinie, S.H. (2008). Predicting the production rate of diamond wire saws in carbonate rock cutting. Industrial Diamond Review. 3: 28-34.
- [10]. Ataei, M., Mikaeil, R., Sereshki, F. and Ghaysari, N. (2012). Predicting the production rate of diamond wire saw using statistical analysis. Arabian Journal of Geosciences. 5: 1289-1295.
- [11]. Ghaysari, N., Ataei, M., Sereshki, F. and Mikaeil, R. (2012). Prediction of Performance of Diamond Wire Saw With Respect to Texture Characteristics of Rock. Archive of Mining Science. 57 (4): 887-900.
- [12]. Sadegheslam, G., Mikaeil, R., Rooki, R., Ghadernejad, S. and Ataei, M. (2013). Predicting the production rate of diamond wire saws using multiple nonlinear regression analysis. Geosystem Engineering. 16 (4): 275-285.
- [13]. Almasi, S.N., Bagherpour, R., Mikaeil, R. and Khademian, A. (2015). Influence of Cutting Wire Tension on Travertine Cutting Rate. 24<sup>th</sup> international mining congress and exhibition of turkey. pp. 1096-1102.
- [14]. Tonshoff, H.K. and Hillmann-Apmann, H. (2002). Diamond tools for wire sawing metal components. Diamond and Related Materials. 11: 742-748.
- [15]. International Society for Rock Mechanics. (1981). Rock characterisation, testing and monitoring: ISRM suggested methods. Oxford: Pergamon.
- [16]. Tercan, A.E. and Ozcelik, Y. (1999). Assessment of Marble Quality in a Dimension Stone Quarry by Geostatistical Methods and Optimum Quarry Planning. Research Fund. Project Number: 98.02.602.004.
- [17]. Ozcelik, Y. (2011). Determination of the regions used as facing and building stone according to the material characteristics in an andesite quarry. Eng Geol. 118: 104-109.
- [18]. Das, S.K. and Basudhar, P.K. (2009). Utilization of self-organizing map and fuzzy clustering for site characterization using piezocone data. Computers and Geotechnics. 36 (1): 241-248.
- [19]. Mikaeil, R., Haghshenas, S.S., Haghshenas, S.S. and Ataei, M. (2016). Performance prediction of circular saw machine using imperialist competitive algorithm and fuzzy clustering technique. Neural Computing and Applications. pp. 1-10.
- [20]. Rad, M.Y., Haghshenas, S.S., Kanafi, P.R. and Haghshenas, S.S. (2012). Analysis of Protection of Body Slope in the Rockfill Reservoir Dams on the Basis of Fuzzy Logic. In IJCCI. pp. 367-373.
- [21]. Haghshenas, S.S., Rad, M.Y. and Haghshenas, S.S. (2013). Evaluation Rock Mass Deformation Modulus based on Fuzzy Logic. 7<sup>th</sup> SASTech.
- [22]. Haghshenas, S.S., Neshaei, M.A.L., Pourkazem, P. and Haghshenas, S.S. (2016). The Risk Assessment of Dam Construction Projects Using Fuzzy TOPSIS (Case Study: Alavian Earth Dam). Civil Engineering Journal. 2 (4): 158-167.
- [23]. Rad, M.Y., Haghshenas, S.S. and Haghshenas, S.S. (2014). Mechanostratigraphy of cretaceous rocks

by fuzzy logic in East Arak, Iran. In Proceedings of 4th international workshop on computer science and engineering. Dubai. (Summer 2014). pp. 45-51.

[24]. Haghshenas, S.S., Haghshenas, S.S., Barmal, M. and Farzan, N. (2016). Utilization of Soft Computing for Risk Assessment of a Tunneling Project Using Geological Units. *Civil Engineering Journal*. 2 (7): 358-364.

[25]. Geem, Z.W. (2000). Optimal cost design of water distribution networks using harmony search. Dissertation. Korea University.

[26]. Geem, Z.W. and Kim, J.H. (2001). Loganathan, A new heuristic optimization algorithm: harmony search. *Simulation*. 76 (2): 60-68.

[27]. The Overview of Harmony Search11. Z.W. (2001). *Music-Inspired Harmony Search Algorithm* Geem (ed.). Springer. Berlin.

[28]. Manjarresa, D., Landa-Torresa, I. and Gil-Lopez, S. (2013). A survey on applications of the

harmony search algorithm. *Eng. Appl. Artif. Intel*. 26 (8): 1818-1831.

[29]. Castelli, M., Silva, S. and Manzoni, L. (2014). Geometric selective harmony search. *Information Sciences*. 279: 468-482.

[30]. Bekdas, G. and Nigdeli, S.M. (2011). Estimating optimum parameters of tuned mass dampers using harmony search. *Eng. Struct*. 33 (9): 2716-2723.

[31]. Miguel, L.F.F. and Kaminski, J.J. (2012). Damage detection under ambient vibration by harmony search algorithm. *Expert Syst. Appl*. 3 (10): 9704-9714.

[32]. Wang, X., Gao, X.Z. and Zenger, K. (2015). *An Introduction to Harmony Search Optimization Method*. Springer Briefs in Computational Intelligence. DOI 10.1007/978-3-319-08356-8\_2. ISBN 978-3-319-08356-8.

## کاربرد الگوریتم جستجوی هارمونی به منظور ارزیابی عملکرد سیم برش های الماسی

رضا میکائیل<sup>۱\*</sup>، ایلماز اوزچلیک<sup>۲</sup>، محمد عطائی<sup>۳</sup> و سینا شفیعی حق شناس<sup>۴</sup>

۱- گروه مهندسی معدن و مواد، دانشگاه صنعتی ارومیه، ایران

۲- دانشکده مهندسی معدن، دانشگاه حاجت تپه، آنکارا، ترکیه

۳- دانشکده مهندسی معدن، نفت و ژئوفیزیک، دانشگاه صنعتی شاهرود، ایران

۴- باشگاه پژوهشگران جوان، دانشگاه آزاد اسلامی واحد رشت، ایران

ارسال ۲۰۱۶/۷/۵، پذیرش ۲۰۱۶/۹/۲۴

\* نویسنده مسئول مکاتبات: reza.mikaeil@uut.ac.ir

### چکیده:

ارزیابی و پیش بینی عملکرد سیم برش های الماسی یکی از فاکتورهای مهم در طراحی و برنامه ریزی معادن سنگ های ساختمانی است. نرخ سایش سیم برش الماسی می تواند به عنوان یکی از معیارهای مهم در ارزیابی عملکرد سیم برش الماسی مورد استفاده قرار گیرد. نرخ سایش سیم برش های الماسی به پارامترهای غیر قابل کنترل نظیر خصوصیات سنگ و پارامترهای قابل کنترل مانند ویژگی های دستگاه برش و پارامترهای عملیاتی وابسته است. در شرایط ثابت عملیاتی، نرخ سایش قویاً تحت تأثیر مشخصات سنگ است. این یک عامل کلیدی است که باید در ارزیابی نرخ سایش سیم برش های الماسی مورد ارزیابی قرار گرفته شود. در این مطالعه، چهار ویژگی عمده سنگ های ساختمانی شامل مقاومت فشاری تک محوری، فاکتور ساینده شیمازک، سختی موس و مدول یانگ به عنوان معیارهای ارزیابی سایش سیم برش های الماسی با استفاده از الگوریتم جستجوی هارمونی انتخاب شدند. الگوریتم جستجوی هارمونی به منظور خوشه بندی پانزده معدن سنگ ساختمانی آندزیتی در کشور ترکیه مورد استفاده قرار گرفته شده است. سنگ های ساختمانی مورد مطالعه در سه دسته مورد ارزیابی و طبقه بندی قرار گرفتند. نتایج حاصل از بررسی ها نشان داد که الگوریتم به کار گرفته شده می تواند برای طبقه بندی عملکرد سیم برش های الماسی از دیدگاه نرخ سایش با توجه به مشخصات فیزیکی و مکانیکی سنگ مورد استفاده قرار گیرد.

**کلمات کلیدی:** سنگ ساختمانی، سیم برش الماسی، نرخ سایش، الگوریتم جستجوی هارمونی.